Structural variations in Z-DNA

P. K. Mandal, S. Venkadesh AND N. Gautham

Abstract | The first crystal structure of Z-DNA, i.e. of the sequence d(CGCGCG)$_2$ established many sequence-dependent micro-structural features. Nevertheless, a regular model of Z-DNA could be built for alternating pyrimidine-purine sequences, with a dinucleotide duplex as the repeating unit, rather than the mononucleotide used in regular models of A and B type helices. In our laboratory, we have made systematic crystallographic studies to explore the precise influence of sequence on the microstructure of Z-DNA, especially the effect of the introduction of A.T base pairs in sequences that otherwise consisted of C.G base pairs. Using chiefly the technique of X-ray crystallography, we studied the following sequences: d(CACGCG).d(CGCGTG), d(CGCACG).d(CGTGCG), d(CACGCG).d(CGCGTG), d(CCCGGG)$_2$, d(CGCGCA).d(TGCGCG), d(CGCGTACGCG)$_2$, and d(CGCGCGTACGCGCG)$_2$.
These sequences were studied under various conditions of salt, pH, temperature, etc. Some of the results we obtained from these studies may be summarized as follows. Firstly, we observe sequence-dependent structural micro-heterogeneities in Z-DNA, which are correlated with the extent of the stretch of G.C base pairs, as well as with the degree and nature of the pyrimidine-purine alternation in the sequence. Secondly, the Z-DNA helices, which may be approximated to solid cylinders, achieve the closest packing in the crystals in the following manner. The cylinders are stacked on top of each other to form long infinite, pseudo-continuous columns, which are then bundled together in a hexagonal close packing arrangement. This packing motif is common to almost all the Z type structures that have been studied, both in our laboratory as well as elsewhere. Despite this common packing principle, it is possible to index the crystals in several different crystals systems and space groups, sometimes in a degenerate manner. The differences arise due to the alignment between adjacent columns. Also if the sequences are non-self complementary, like many of those above, the helical columns can point 'up' or 'down' and this allows an extra degree of freedom in choice of crystal system and space group. The third set of results obtained from these studies pertains to the interactions of various metal ions with the helices. We find, in particular, that cobalt and ruthenium hexammine ions perturb the tautomeric state of the adenine and thymine bases, leading to changes in the base pairing schemes.

Centre of Advanced Study in Crystallography and Biophysics, University of Madras, Guindy Campus, Chennai 600025, India
n_gautham@hotmail.com

Introduction

DNA is thought to encode biological information in two ways (Dickerson, 1992; Herbert and Rich, 1996) — via the sequence, and via the structure. The first, and the most obvious way, is through the linear sequence of bases that

may code for proteins, or may act as sites of chemical recognition for regulatory proteins or other molecules. The second way is through the particular three-dimensional structure of the DNA helix that interacts specifically with proteins and other molecules. While even in this latter case the information is still coded in the sequence, the expression of this information is through modulations in the structure of the DNA, rather than by direct chemical recognition. Such modulations may be again classified in two ways. The structure of DNA is usually the well-known Watson-Crick right-handed B type double helix. However, under certain conditions it departs noticeably from this in a sequence-dependent manner. For example, sequences that have purine repeats appear to prefer the A type double helix (McLean *et al.*, 1986). Another, more dramatic, instance of sequence-specific structure is the left-handed Z type structure, preferred by alternating pyrimidine-purine repeats, in particular CG repeats. A second type of sequence dependent modulation of DNA structure is the local structural microheterogeneity displayed by the helix. Thus, while early models of DNA helices (Watson and Crick, 1953; Franklin and Gosling, 1953; Langridge *et al.*, 1957) have the same regular structure repeated from base pair to base pair throughout the helix, detailed structures obtained by X-ray crystallography and NMR studies of oligonucleotides show variations in the structure that are related to the sequence. Such variations have been documented extensively for right-handed helices such as B type DNA (Wing *et al.*, 1980). In this review we discuss structural variations seen in left-handed DNA.

In 1972 Pohl and Jovin noted an inversion of the CD spectrum of an alternating synthetic copolymer poly (dG-dC).poly (dG-dC) in highly concentrated salt solution (Pohl and Jovin, 1972), consistent with a change in the structure from a right-handed to a left-handed helix. A few years later, in 1979 Rich and co-workers solved the X-ray crystal structure of $d(CpGpCpGpCpG)_2$ (Wang *et al.*, 1979). The structure revealed that the hexanucleotide DNA fragment assumed a left-handed helical structure containing Watson-Crick base pairing (Figure 1). The structure was further characterized by an alternation in some of the helical parameters, such as sugar puckering, conformation about the glycosidic torsion angle, and some of the backbone torsion angles. One of the consequences of this alternation was that the sugar-phosphate chain that forms the backbone of the DNA helix proceeds in a zigzag fashion, leading to the name Z-DNA for this helix.

This crystal structure led to a great deal of scientific effort to characterize the DNA sequences

Figure 1: The structure of $d(CGCGCG)_2$

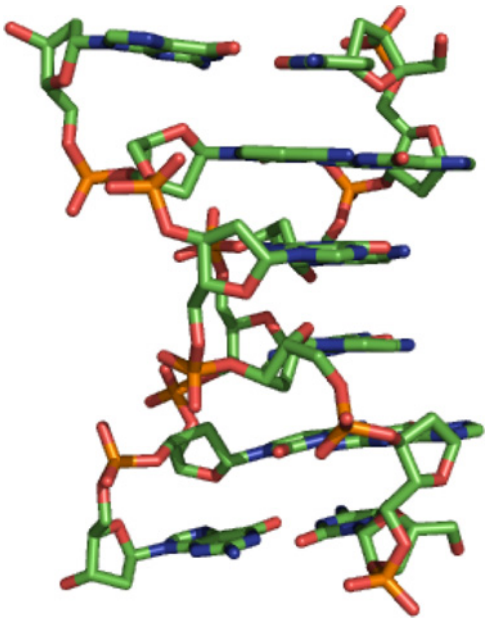

and environmental conditions required for Z-DNA formation. It was shown that Z-DNA can be stabilized by Z-helical DNA binding proteins, chemical modifications, methylation, monovalent and divalent cations and DNA negative super coiling (Peck *et al.*, 1982; Singleton *et al.*, 1982; Sinden, 1994). The discovery of Z-DNA is important because the ability of DNA to adopt non-Watson-Crick structures could have profound implications for the processes of replication, recombination, and transcription (Sinden, 1994). However, direct evidence for the existence of left-handed DNA *in vivo* has been difficult to obtain, perhaps because less than 1% of natural genomic ds-DNA is capable of adopting the Z-helical conformation (Jaworski *et al.*, 1987), though, within human genes a larger percentage of potential Z-DNA forming sequences can be quantified, ranging from about 35% to 62% (Schroth *et al.*, 1992).

Both Z-DNA and B-DNA are double-stranded, with the two strands arranged anti-parallel on the outside of the helix. The bases attached to the two strands make Watson-Crick hydrogen-bonded base-pairs, and are arranged on the inside of the helix. However there are a number of differences between the B-DNA and Z-DNA. The most obvious one is, of course, the helical sense, which is right-handed in B DNA and left-handed in Z-DNA. Table 1 lists some of the other structural differences, and Figure 2 illustrates these.

The parameters given in the table for both helical types are obtained from fibre diffraction

Figure 2: Regular models of the B type and Z type helices derived from fibre diffraction data.

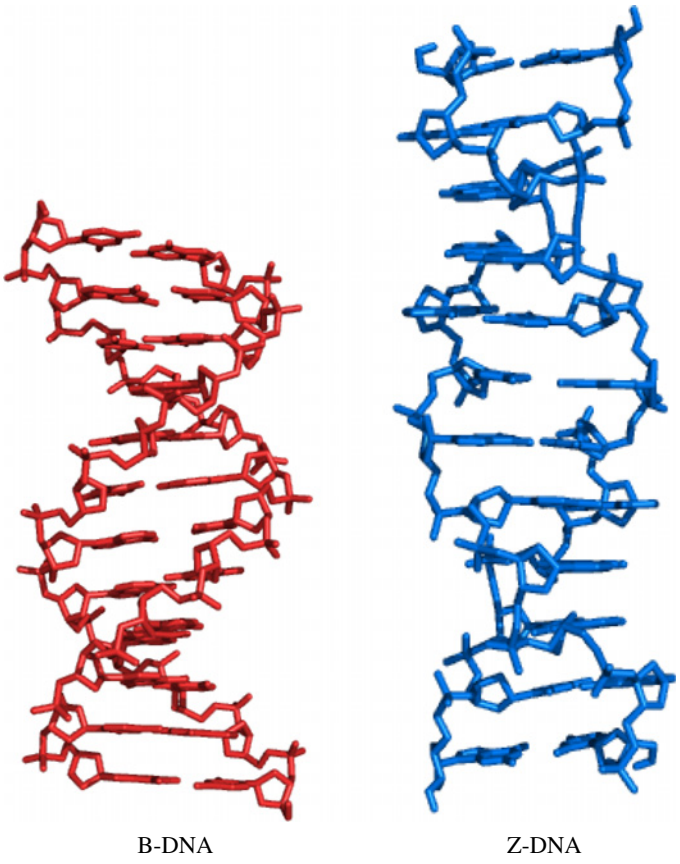

Table 1: Structural differences between B-DNA and Z-DNA.

Parameters	B-DNA	Z-DNA
Residues per turn	10.5	12
Axial rise (Å)	3.24	3.72
Helix pitch (Å)	34	45
Base pair tilt (°)	-6	7
Rotation per residue (°)	36	-30
Diameter of helix (Å)	~20	~18
Glycosidic bond configuration: dA, dT, dC dG	*anti* *anti*	*anti* *syn*
Sugar pucker: dA, dT, dC dG	C2′ endo C2′ endo	C2′ endo C3′ endo
Intrastrand phosphate- phosphate distance (Å): dA, dT, dC dG	 7.0 7.0	 7.0 5.9
Repeating base pair unit	One	Two
Grooves: Major Minor	Wide and deep Narrow and deep	Flat Narrow and deep

studies, or from uniform models built to explain X-ray data. With the availability of a large number of single crystal structures of oligodeoxynucleotides since the early 1980s, sequence-dependent microheterogeneities in the double helical structure became apparent. Studies by many workers (Wing *et al.*, 1980; Drew *et al.*, 1981; Drew and Dickerson, 1981) established several

features regarding structural flexibility and plasticity in B type helices. The sequence-dependence of these features was also demonstrated.

The first crystal structure of Z-DNA, i.e. of the sequence d(CGCGCG)$_2$ (Wang *et al.*, 1979) established the following sequence-dependent micro-structural features: Two types of backbone conformations; different stacking interactions at the CpG base steps as compared to the GpC base steps; differing orientations about the glycosidic bond – *syn* and *anti* for dG and dC bases, respectively; and different puckering modes – *C3′-endo* and *C2′-endo* for dC and dG nucleotides respectively. However, a regular model of Z-DNA could be built on the basis of these studies, as well as of those carried out on fibers of synthetic polynucleotides with alternating pyrimidine-purine sequences. This model has a dinucleotide duplex as a repeating unit, rather than

Figure 3: Two possible regular models for Z DNA based on different backbone structures (i) Z_I and (ii) Z_{II}.

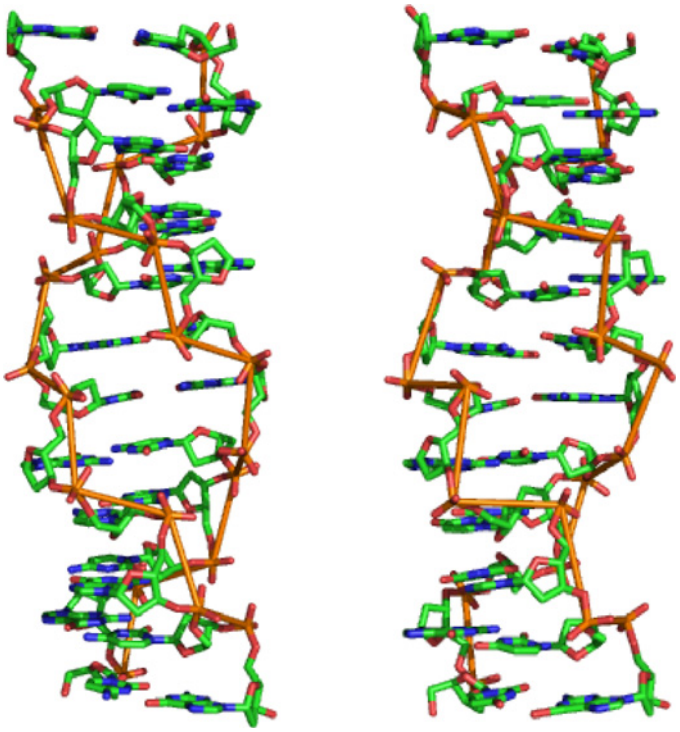

Figure 4: Three different non-self complementary duplexes resulting from the replacement of a G:C base pair by an A:T base pair in d(CGCGCG)$_2$.

5’ C1 G2 C3 G4 C5 G6 3’		d(CGCGCG)$_2$
3’ G12 C11 G10 C9 G8 C7 5’		
5’ C1 A2 C3 G4 C5 G6 3’		HA2
3’ G12 T11 G10 C9 G8 C7 5’		
5’ C1 G2 C3 A4 C5 G6 3’		HA4
3’ G12 C11 G10 T9 G8 C7 5’		
5’ C1 G2 C3 G4 C5 A6 3’		HA6
3’ G12 C11 G10 C9 G8 T7 5’		

Figure 5: Stereo view of the structure of the HA2 sequence d(CACGCG).(CGCGTG). The A.T base pair is marked in blue.

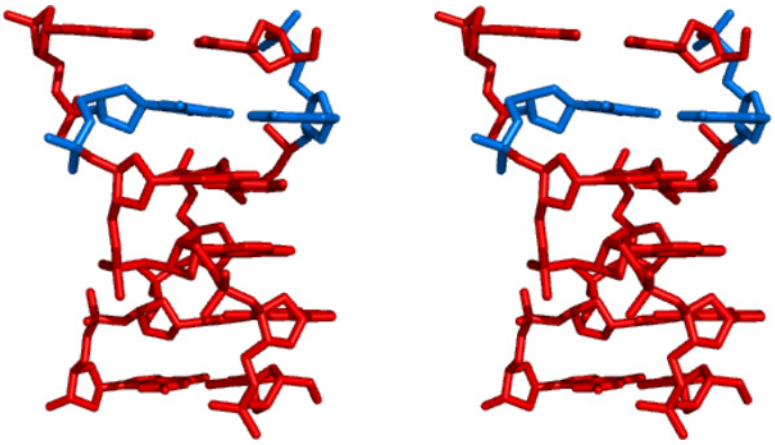

Figure 6: Least squares superposition diagram of HA2 (yellow) on d(CGCGCG)$_2$ (blue).

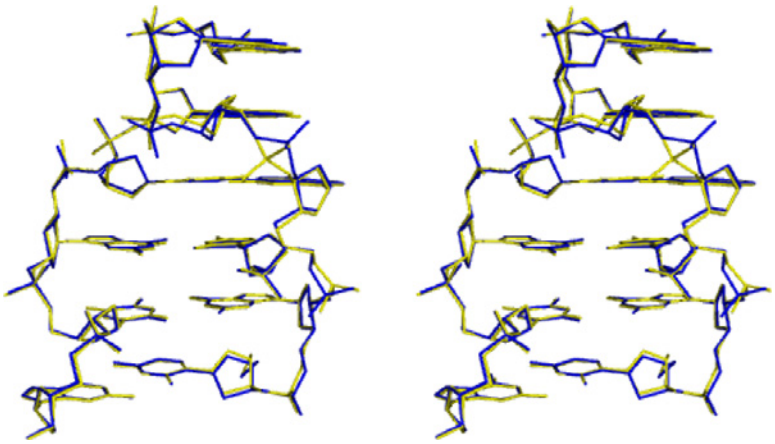

the mononucleotide used in regular models of A and B type helices. In fact, as shown in Figure 3, there are two possible regular models for Z DNA – one with the so-called Z_I type backbone structure and the other with a Z_{II} type backbone structure (Ho and Mooers, 1997; Harper *et al.*, 1998; Subirana and Solar-Lopez, 2003).

Z-DNA forms readily in alternating pyrimidine-purine sequences; $(CG)_n$ sequences take up this structure most easily (Pohl and Jovin, 1972; Wang *et al.*, 1979; Drew *et al.*, 1980; Crawford, 1980; Jayaraman and Yathindra, 1981; Sutherland *et al.*, 1981). $(TG)_n$ sequences also form Z-DNA but they require greater stabilization energy (Sinden, 1994). Though $(TA)_n$ sequences easily form cruciform structures, two conditions favour Z-DNA formation, namely, introduction of up to ten alternating T.A base pairs embedded in a stretch of $(CG)_n$, and conditions of high negative super coiling or high salt(Klysik *et al.*, 1988). Chemical modifications like bromination or methylation at the C5 position of cytosine or the C8 position of the guanine allows stabilization of Z-DNA at lower salt concentration (Fujii *et al.*, 1982; Möller *et al.*, 1984; Chevrier *et al.*, 1986). Methylation at the N7 position of guanine also favors the Z-form (Rich *et al.*, 1984; Chevrier *et al.*, 1986). Sequences other than alternating purines and pyrimidines also form Z-DNA. The ease with which this occurs depends on the sequence. For example, a $d(GGGC)_n$ repeat adopts the Z structure more readily than $d(TA)_n$ (Herbert and Rich, 1996).

In the past decade in our laboratory, we have made systematic crystallographic studies to explore the precise influence of sequence on the

Figure 7: Stereo view of the structure of the HA4 sequence d(CGCACG).(CGTGCG). The A.T base pair is marked in blue.

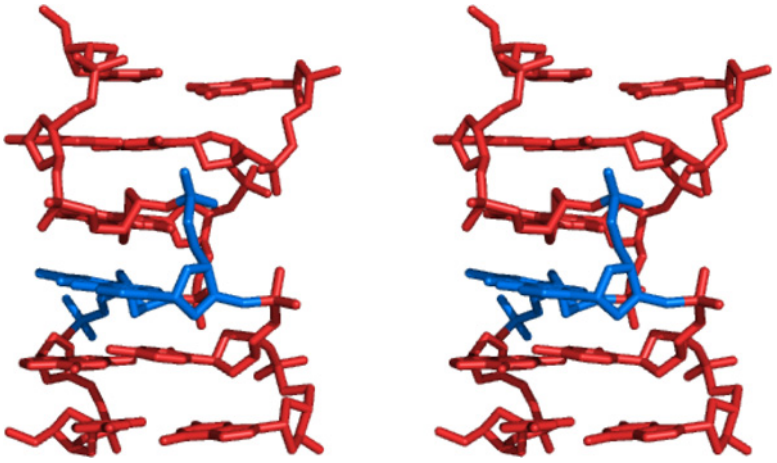

Figure 8: Least squares superposition diagram of HA4 (yellow) on d(CGCGCG)$_2$ (blue).

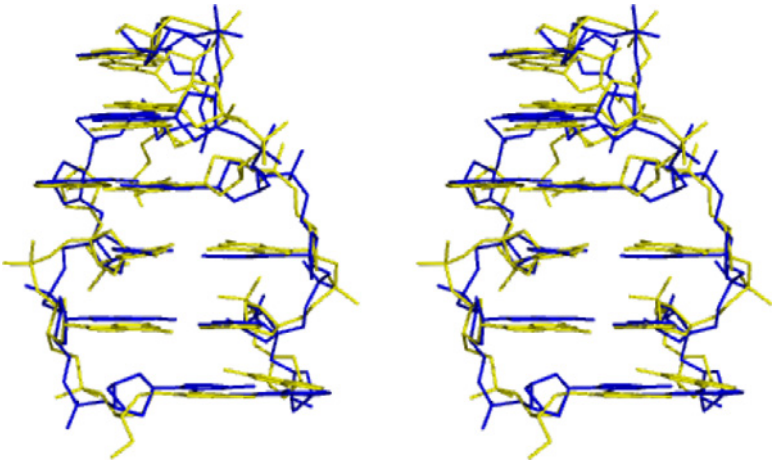

microstructure of Z-DNA. In particular we have studied the effect of the introduction of A.T base pairs in sequences that otherwise consisted of C.G base pairs. The design of the sequences we studied was based primarily upon the canonical hexamer d(CGCGCG)$_2$. Since this sequence is self-complementary, the duplex has a dyad, and there are only three ways in which a single A:T base pair could replace one of the G:C pairs, and three ways in which a CG or GC dinucleotide is replaced by a TA or AT dinucleotide. Figure 4 illustrates these possibilities. We have studied all three possibilities in various conditions of salt, pH, temperature, etc. We have also studied decamer and tetradecamer sequences that adopt the Z form helix. A list of all the structures reviewed in the present paper is given in Table 2. We first discuss the structural differences in these sequences as compared to each other, as well as to structure of the canonical Wang and Rich sequence d(CGCGCG)$_2$ and to the fibre model. In the subsequent section we discuss certain interesting aspects of the packing of short DNA helices in crystals. In the final section we review the structural aspects of the interactions of metal ions with the DNA helices.

Sequence dependent structure

Depending on the position of the AT base pair replacement in the duplex d(CGCGCG)$_2$, the new sequences are termed HA2, HA4, and HA6, referring

Figure 9: Schematic representation of twist angles in HA2 and HA4. Each bar represents a base pair. For clarity, only one base of each pair is marked.

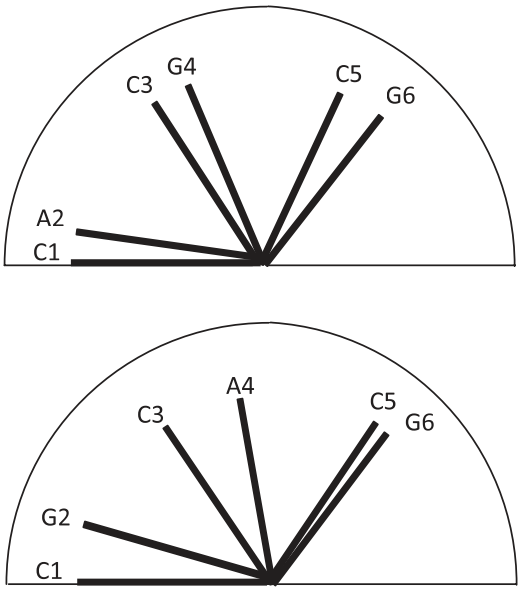

to the second, fourth, and sixth positions for the adenine base (and correspondingly the fifth, third, and first positions for the complementary thymine base). The different substitutions result in variation of the extent of the G:C tract in the canonical hexamer. Crystals of HA2 were grown in the presence of magnesium chloride. The structure was obtained at a resolution of 1.60 Å and refined to an R factor of 19.9%. This structure (Figure 5) is almost identical to the regular structure of Z-DNA. Figure 6 shows a superposition of HA2 on the structure of $d(CGCGCG)_2$ (Wang *et al.*, 1979). It is clear that in this case the AT base pair has almost negligible effect on the structure. The helical rise and twist of base pairs are almost the same as the standard values. There is no noticeable difference in the stacking interactions of the A.T base pair as compared to the G:C base-pairs. The four purine-pyrimidine steps in HA2 adopt the Z_I conformation, i.e., the torsion angles ζ and α at the phosphodiester linkage are *gauche*$^-$ and *trans* respectively (Sadasivan and Gautham, 1995). The glycosyl torsion angles, χ, of HA2 take up the expected alternate *anti* and *syn* orientations (Sadasivan and Gautham, 1995).

Crystals of HA4 were grown in the presence of barium chloride. This sequence crystallized in the space group $P2_1$. The structure could be refined to $R = 16.1\%$ with data to a resolution of 2.5 Å (Figure 7). The molecule possesses a dinucleotide repeat with an average left-handed twist of $-57°$ per dinucleotide, close to the standard value. Figure 8 shows a superposition of HA4 on the structure of $d(CGCGCG)_2$ (Wang *et al.*, 1979). It is clear that the despite the overall structure being similar there are many differences. One of these differences is that the twist does not alternate uniformly. Some of the steps are underwound, and some are overwound. This is made clear in Figure 9 which is a 'speedometer dial' view of the twist values in HA2 and HA4. In the latter structure the C3pA4/T9pG10 step is highly overwound (twist angle $-24°$) and the C5pG6/C7pG8 step is highly underwound (twist angle $-3.17°$). Figure 10 compares the stacking patterns at these steps in HA4 with those at equivalent steps in HA2 and in $d(CGCGCG)_2$. The variations from regularity in the twist angle mentioned above are reflected in the patterns of stacking of adjacent base pairs. The average rise per base pair (3.58 Å) is less than the standard value of 3.72 Å. A large part of this compression of the helix occurs in the dinucleotide steps at the two ends. Many of the backbone torsion angles are noticeably different from those of other Z-DNA structures. The difference is greater at the first and last pyrimidine-purine steps than in central region of the molecule. The values of the torsion angles ζ and α at the phosphodiester linkage in all the steps are substantially different from the previously obtained values. For the glycosyl torsion angle χ, the average values are close to those expected for Z-DNA, but the variation in χ is greater than in the standard structure. The sugar puckering does not

Table 2: Sequences discussed in this review with their crystal data [all datasets collected at room temperature (300K)].

Sl. No	NAME	Sequence	Space group	Cell parameters	Res. (Å)	NDB ID	Reference
1	HA2_Mg	d(CACGCG).d(CGCGTG)	$P2_12_12_1$	a = 17.76 Å b = 30.96 Å c = 44.75 Å	1.60	ZDF039	Sadasivan and Gautham, 1995
2	HA2_Ru	d(CACGCG).d(CGCGTG)	$P2_12_12_1$	a = 17.88 Å b = 30.87 Å c = 44.83 Å	1.64	ZDF059	Bharanidharan *et al.*, 2007
3	HA4	d(CGCACG).d(CGTGCG)	$P2_1$	a = 17.75 Å b = 17.76 Å c = 42.77 Å $\gamma = 120.05^{\circ}$	2.50	ZDF038	Sadasivan *et al.*, 1994, Sadasivan and Gautham, 1995
4	C3G3	d $(CCCGGG)_3$	$P2_12_12_1$	a = 17.76 Å b = 30.94 Å c = 43.92 Å	2.05	ZDF049	Karthe, *et al.*, 1997
5	OHA6_Co	d(CGCGCA).d(TGCGCG)	$P2_12_12_1$	a = 17.98 Å b = 30.93 Å c = 44.63 Å	1.71	ZD0013	Thiyagarajan *et al.*, 2004, 2005
6	HHA6_Co	d(CGCGCA).d(TGCGCG)	$P6_5$	a = 35.59 Å b = 35.59 Å c = 44.52 Å	2.00	ZD0014	Thiyagarajan *et al.*, 2004, 2005
7	OHA6_Ru	d(CGCGCA).d(TGCGCG)	$P2_12_12_1$	a = 17.95 Å b = 30.84 Å c = 44.60 Å	1.54	ZD0017	Bharanidharan *et al.*, 2007
8	HHA6_Ru	d(CGCGCA).d(TGCGCG)	$P6_5$	a = 35.89 Å b = 35.89 Å c = 44.60 Å	2.60	ZD0018	Bharanidharan *et al.*, 2007
9	DTA56	$d(CGCGTACGCG)_2$	$P6_5$	a = 31.13 Å b = 31.13 Å c = 43.22 Å	2.15	–	Unpublished results
10	TDTA78	$d(CGCGCGTACGCGCG)_2$	$P3_2$	a = 31.33 Å b = 31.33 Å c = 44.72 Å	2.50	–	Unpublished results

strictly follow the pattern of alternation between C3′-endo and C2′-endo. Nor does it follow the pattern observed in $d(CGCGCG)_2$, or in HA2 (Sadasivan and Gautham, 1995).

The crystals of HA2 and HA4 were grown at nearly the same conditions. Yet, a relatively small change in the sequence appears to cause a fairly large change in the structure. These results lead us to the following possible conclusions. Firstly, though Z-DNA is far more tightly wound than either the A type or the B type helices, left-handed DNA can also show microheterogeneity in its structure (similar to the right-handed helices), and that these structural variations are probably correlated with the sequence. Secondly, more than one form of left-handed DNA is possible. And thirdly, in order to form a stable, regular left-handed Z type structure, it is required not only to have an alternating pyrimidine-purine sequence, but also a stretch of at least four G.C base pairs. This last conclusion follows from the fact that HA2 has such a stretch of four G.C base pairs, while HA4 does not. Further support for these conclusions were obtained from the structures of HA6 and $d(CCCGGG)_2$

The HA6 sequence was crystallized in the presence of cobalt hexammine chloride at two different concentrations. With 0.5 mM cobalt hexammine chloride and 0.05 mM spermine in the crystallization solution, crystals grew in the orthorhombic space group $P2_12_12_1$. The crystals diffracted to a resolution of 1.71 Å. The structure was solved and refined to R = 20.8% (Figure 11). This sequence adopts the 'canonical' Z DNA structure. This is evident from Figure 12, which is a superposition of the HA6 (orthorhombic) helix on $d(CGCGCG)_2$. The only distinct change in HA6 from the fibre model is the Z_{II} type backbone structure at residues C5 and C9. The backbone angles ζ and α have the conformation *gauche*$^+$, *trans* at these residues, instead of the *gauche*$^-$, *trans* conformation found in the regular fibre-derived model. The Z_{II} conformation has also been seen in the structure of $d(TGCGCA)_2$ (Harper *et al.*, 1998; Thiyagarajan *et al.*, 2002) in which the backbone has the Z_{II} conformation at the three residues C3, C9 and C11. In HA6, the Z_{II} conformations at C9 and C5 could be related to interactions of the phosphate groups with the cobalt hexammine

Figure 10: Stacking of adjacent bases in d(CGCGCG)$_2$, HA2 and HA4. A.T base pairs are marked in red. The first, second and third columns consist of the bases of the hexamers d(CGCGCG)$_2$, HA2 and HA4, respectively.

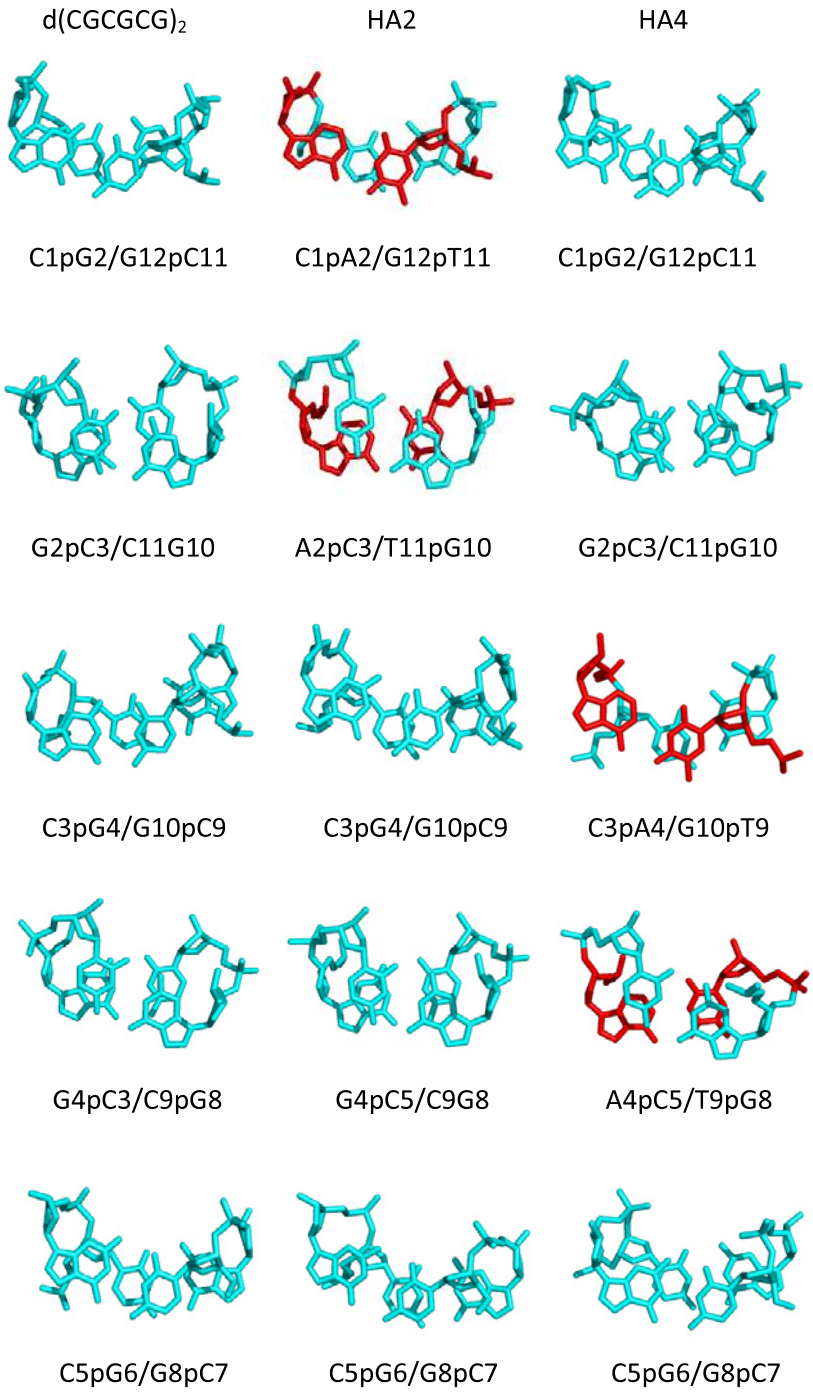

ion. However this idea has no support from the crystals of HA6 that were grown with ruthenium hexammine in the crystallization solution. This structure, obtained at resolution 1.54 Å and refined to R factor 18.9% is very similar in conformation and crystal packing to that of HA6 grown with cobalt hexammine. A noticeable feature of the ruthenium structure is the backbone conformation at the residues C3, C5, C9 and C11, which is a mixture of the Z_I and the Z_{II} conformations at each

Figure 11: Stereo view of the structure of the HA6 sequence d(CGCGCA).(TGCGCG) in the orthorhombic space group (i.e. OrthHA6).

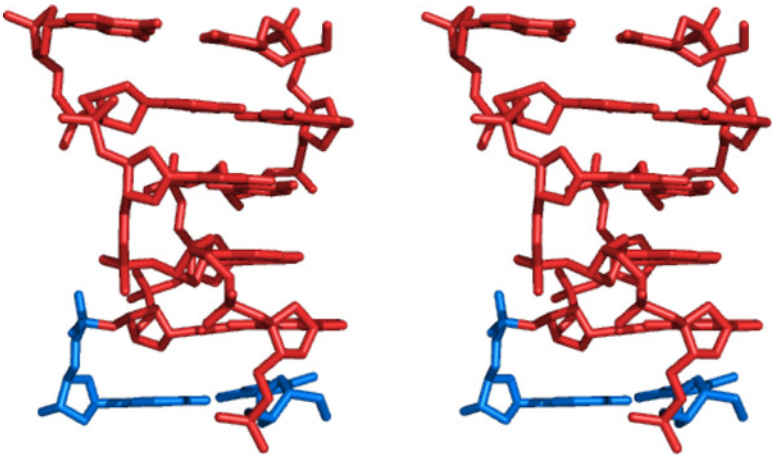

Figure 12: Least squares superposition diagram of HA6 (yellow) on $d(CGCGCG)_2$ (blue).

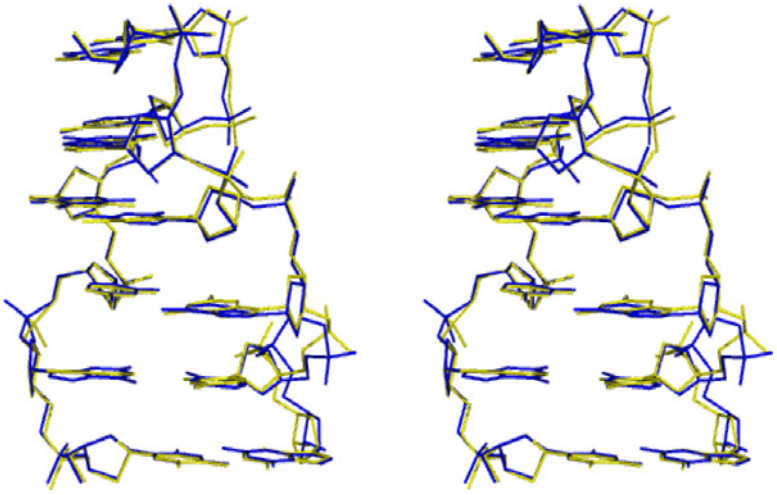

of these residues. Two of these phosphate groups, viz. C3 and C5, interact directly with the ruthenium hexammine ion. The phosphate at C11 makes only indirect, water-mediated interactions with the ion, while the backbone atoms at C9 have no such interaction. Thus the Z_I and Z_{II} conformations are specific neither to the sequence, nor to the metal ion interactions.

When the concentration of the metal ion in the crystallization solution was lowered, with both cobalt hexammine and with ruthenium hexammine, the crystals grew in the hexagonal space group $P6_5$. The asymmetric unit in this case consisted of a hexamer duplex and a dimer duplex, both of which are very similar to the standard Z-DNA helix. (The packing interactions between the duplexes in these crystals are different from the orthorhombic case and are discussed in a later section.) This sequence has five consecutive C.G base pairs, arranged in alternation, and the structures, both in the orthorhombic space group as well as in the hexagonal space group, and both in the presence of cobalt hexammine as well as in the presence of ruthenium hexammine, lend support to the idea that four alternating C.G pairs are required for stable Z-DNA. It must however be borne in mind that cobalt hexammine is a strong inducer and stabilizer of the Z type helix, and the occurrence of 'canonical'

Figure 13: Stereo view of the structure of $d(CCCGGG)_2$.

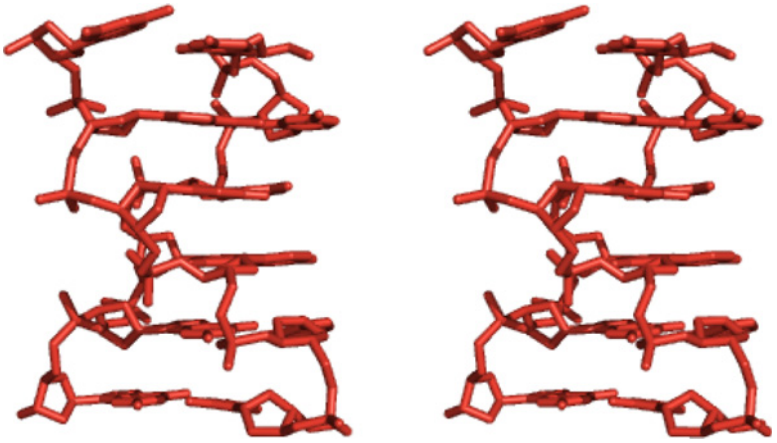

Figure 14: Schematic representation of twist angles in $d(CCCGGG)_2$. Each bar represents a base pair. For clarity, only one base of each pair is marked.

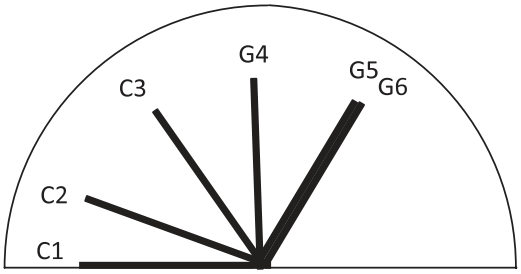

conformation may not be only sequence-dependent. Details of the ion interactions are discussed in a later section.

The non-alternating sequence $d(CCCGGG)_2$ also crystallizes as left-handed DNA (Figure 13) (Gautham *et al.*, 1999). However the helical parameters are quite different from standard Z-DNA values. Figure 14 is a 'speedometer dial' view of the twist values in this structure. The four central base pairs, including the single pyrimidine-purine step, possess uniform twist values, unlike the alternating pattern seen in the standard structure. The twist values at the two ends of the helix do not follow this pattern of uniformity, but are also different from the average values observed previously in Z-DNA. The values of the other parameters, too, are uniform in the central portion of the helix. These four central base-pairs may be used to construct a uniform, non-alternating model of left-handed DNA, different from Z DNA (Figure 15). The glycosyl torsion angles (χ), broadly follow the standard alternating *syn* and *anti* pattern, although the angles vary over a wide range from low *anti* to high *syn*. The sugar moieties exhibit a wide range of puckering modes, from C3′-endo to O4′-exo. The backbone torsion angles deviate from previously observed values throughout the structure. From the point of view of sequence-dependent structure, this sequence indicates that a stretch of four G.C base pairs, while necessary, is not sufficient to nucleate standard Z DNA – these base pairs have to also alternate in sequence. However, the single CG base pair at the centre of the sequence appears sufficient, together with high salt concentration and possible packing interactions, to drive the duplex into a quasi-uniform left-handed helix. The lack of high resolution data from these crystals prevented a more detailed categorization of this helix.

The decamer sequence $d(CGCGTACGCG)_2$ also crystallizes as left-handed Z DNA. Magnesium chloride was present in the crystallization solution as the counter ion. The crystal diffracted up to

Figure 15: A polymorph of Z-DNA with uniform twist. The central tetramer $(CCGG)_2$ of the structure of $d(CCCGGG)_2$ was used to generate this helix.

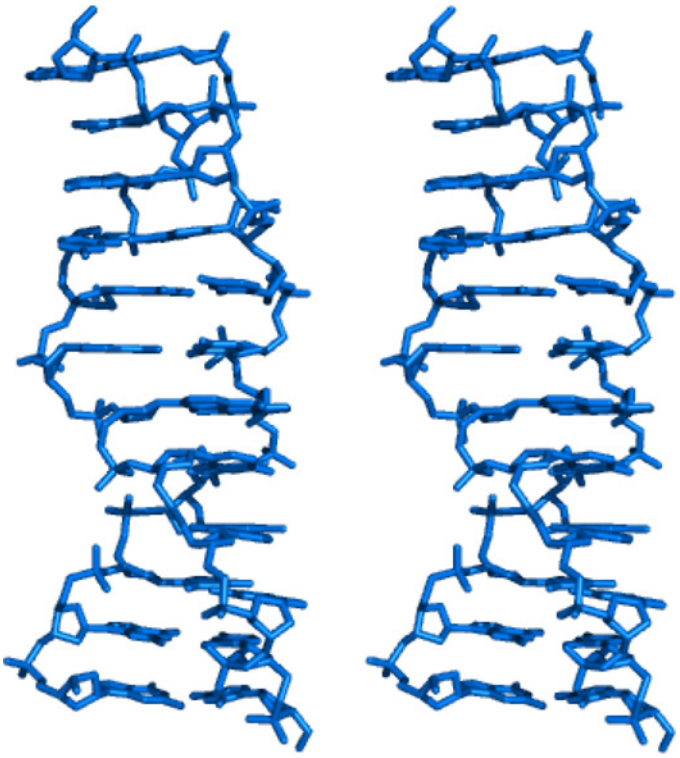

a resolution of 2.15 Å in the space group $P6_5$. The crystallographic asymmetric unit contains two helices, and both of them are positioned on symmetry axes in the crystal. One of the helices is constituted by a tetramer, nominally $d(TGTG)_2$, positioned on the three-fold screw axis. The operation of the three-fold screw gives rise to the dodecamer, with its helix axis parallel to the c axis of the unit cell. The other helix is constructed from a dimer, nominally $d(TG)_2$, placed on the six fold screw axis. In the next section we discuss the details of these packing modes, and the effect they have on the atomic occupancy factors. Here we remark that, as may be seen from Figure 16, the structures follow the standard Z-helical model very closely, and show no discernible variations at the A.T base pairs. According to the hypotheses we have discussed above, this is probably not surprising, since the sequence consists of two tracts of four C.G bases flanking the two A.T base pairs, with continuous pyrimidine-purine alternations.

The tetra-decamer sequence $d(CGCGCGTACG-CGCG)_2$ consists of two tracts six C.G base pairs flanking two A.T base pairs in the centre, again with continuous pyrimidine-purine alternation. Once again it is no surprise that this sequence also prefers to crystallize as a standard Z form helix. Crystals of this sequence were grown in the presence of magnesium sulphate. The crystals diffracted up to 2.5 Å and the data set was indexed in space group $P3_2$. Since the one complete turn of Z-DNA consists of 12 base pairs, the packing mode of the 14-mer helix, just as for the 10-mer helix above, is of interest. This is discussed in the next section.

To conclude this section, we observe that the sequences crystallized and solved in our laboratory yield evidence regarding sequence-dependent structural micro-heterogeneities in Z-DNA. These structural modulations are correlated with the extent of the stretch of G.C base pairs, as well as with the degree and nature of the pyrimidine-purine alternation in the sequence. Packing interactions and the influence of metal ions are also important determinant of the microstructure, and are discussed in the following sections.

Crystal packing

DNA helices, and in particular Z-DNA helices may be approximated to solid cylinders. It is well known (Weaire, 1996) that the closest packing that such cylinders can achieve is the following

Figure 16: Crystal structure of d(CGCGTACGCG)$_2$. The asymmetric unit consists of the tetramer (TGTG)$_2$ and dimer (TG)$_2$. (a) A 12-mer generated by the application of the crystallographic 3-fold to the tetramer. (b) A 12-mer generated by the application of the crystallographic 6-fold to the dimer.

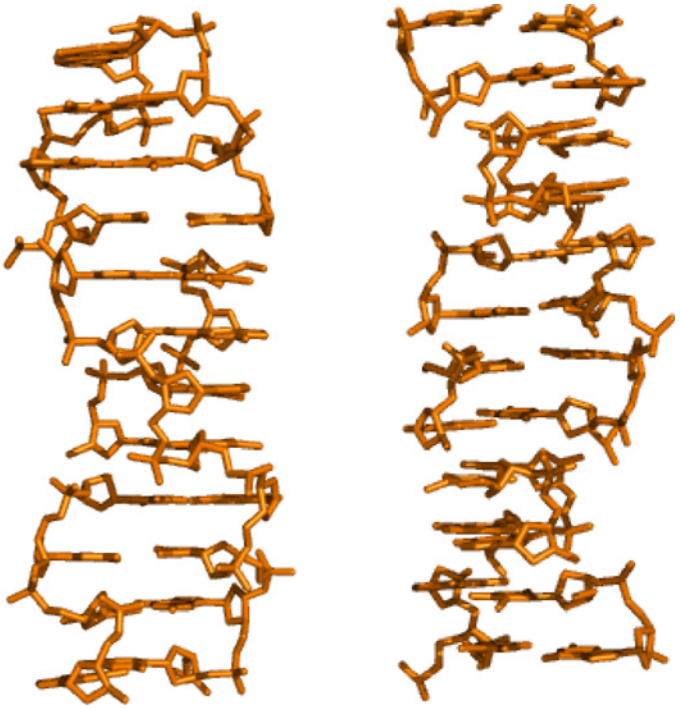

(a) (b)

(Figure 17). The cylinders are stacked on top of each other to form long infinite, pseudo-continuous columns, which are then bundled together in a hexagonal close packing arrangement. If the bundles of cylinders packed in this fashion are considered as crystals, then it is possible to index these in several different crystals systems and space groups (Figure 18), sometimes in a degenerate manner (Sadasivan *et al*., 1994).

Z-DNA helices are only approximately cylinders, and their packing in crystals is actually degenerate only at low resolution. At resolution better than about 2.0 Å it is usually easily possible to assign a single correct crystal system, unit cell and space group. However differences in the sequence, in the crystallization conditions, in the length of the helix and in the metal ion interactions lead to small differences in the inter-helical contacts, which in turn lead to different cells and space groups, all of which however fall within the general packing modes for cylinders as described above. One complete turn of the Z type helix is about 45 Å long (Wang *et al*., 1981), and this is usually the length of the longest axis of the unit cell in Z DNA crystals. If the molecule is a hexamer, then we have two duplexes stacked on each other along this long axis in each unit cell. Crystals of DNA sequences of other lengths (8-mers, 10-mers and 14-mers) have approximately the same long axis length, but accommodate the duplex in different ways, as described below. The other two axes are usually about 17 Å, corresponding to the width of the Z type helix, or multiples of this number. If the packing viewed down the long axis is not perfectly hexagonal close packed (as for example in the orthorhombic space groups), one of the axes lengths then increases to a value between 17 and 34 Å.

A different type of packing was observed in a tetramer sequence d(CGCG)$_2$ (Drew *et al*., 1978) with high salt ion concentrations. Here the duplexes forming the infinite columns are tilted with respect to the column axis, and the columns are curved. Such packing crystal may be indexed in either an orthorhombic or a monoclinic space group. Similar packing was also observed in the hexamer d(pCGCGCG) (Malinina *et al*., 1998) which has an intact phosphate group at the 5′ end. This sequence was crystallized in two space groups, orthorhombic C222$_1$ and monoclinic P2$_1$. The sequence d(CGTACG)$_2$(Parkinson *et al*., 1995) is one of the few examples of left-handed DNA which does not follow the pattern of 'bundles of columns

Figure 17: Close packing of cylindrical objects – general mode.

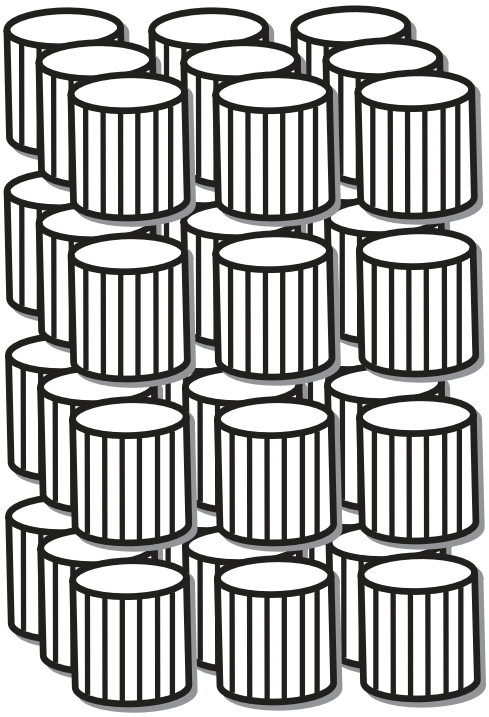

of helices'. It crystallized in the trigonal space group $P3_221$. The hexamer helices are packed almost perpendicular to each other, with the terminal CG base pair of one duplex stacking against the shallow major groove of the adjacent hexamer. This packing is reminiscent of A-DNA crystals.

Such packing modes are however rare, and most of the crystals grown in our laboratory follow the general principles involved in packing Z type helices as described above. In the following paragraphs we describe some specific examples.

Figure 19 shows the packing of the hexamer HA2 in the unit cell, with views both down the long axis, and well as perpendicular to it. The space group is orthorhombic $P2_12_12_1$, just as in the structure of the 'canonical' sequence $d(CGCGCG)_2$ (Sadasivan and Gautham, 1995). However, the single A.T base pair present in HA2, with sequence d(CACGCG).d(CGCGTG), destroys the 2-fold symmetry perpendicular to the helix axis which is present in self-complementary DNA sequences. As a consequence of this, there are two orientations of the HA2 helix with respect to the *c* axis, parallel and anti-parallel. We note that this packing arrangement cannot be indexed, for example, in the hexagonal system for two reasons. The first is that, as for $d(CGCGCG)_2$, adjacent columns of helices are not in register with each other, and the base pairs at the ends of the duplexes in adjacent columns are not in the same plane. The second is that in HA2 the adjacent helices are related by a two-fold axis perpendicular to the long axis. It may be noted that, though both crystals of HA2 as well as of $d(CGCGCG)_2$ are best indexed in orthorhombic $P2_12_12_1$, in the latter each column of helices itself possesses a perpendicular two-fold axis.

HA4 crystallizes in $P2_1$, with c as the unique axis (Figure 20). The unique angle γ is 120.05° nearly the value required for a hexagonal cell. In this structure the terminal base-pairs are all in the same *ab* plane. This feature also could have facilitated the indexing of the cell in a hexagonal space group. This, however, has been prevented by the molecule lacking the perfect six-fold screw symmetry along the helix axis which would be required in the hexagonal cell, since the helical column would then be placed on the crystallographic six-fold axis. With two duplexes in the cell placed one on the other, the column is correctly positioned on the 2_1 screw axis, accommodating the $P2_1$ space group.

As described earlier, crystals of HA6 grew in two slightly different morphologies, corresponding to slight differences in the concentration of the cobalt hexammine ion in the crystallization solution. These two forms were indexed in two different space groups, namely orthorhombic $P2_12_12_1$ and

Figure 18: Crystal system variations in crystals of cylindrical objects. (a) The ends of the cylinders in adjacent columns are in the same *ab* plane. The possible systems are monoclinic, orthorhombic or hexagonal. (b) The ends of the cylinders in adjacent columns are not in the same *ab* plane. The possible systems are monoclinic or orthorhombic. (c) In non-selfcomplementary sequences, the cylinders in adjacent columns are arranged anti-parallel to each other. The arrow indicates the direction of the cylinder. The possible system is orthorhombic. (d) In non-selfcomplementary sequences, the cylindrical columns in adjacent columns are arranged in parallel to each other. The arrow indicates the direction of the cylinder. The possible systems are monoclinic or hexagonal. (e) The ends of cylinders are in same *ab* plane, but the cylinders are stacked in opposite direction. Such packing leads to C centering. (f) The packing of hexamers in hexagonal lattice. In the first and third columns, the hexamer is placed on 2-fold screw axis, two hexamers complete one turn. In the second column, the dimer is placed on 6- fold screw axis, six dimers complete one turn per helix.

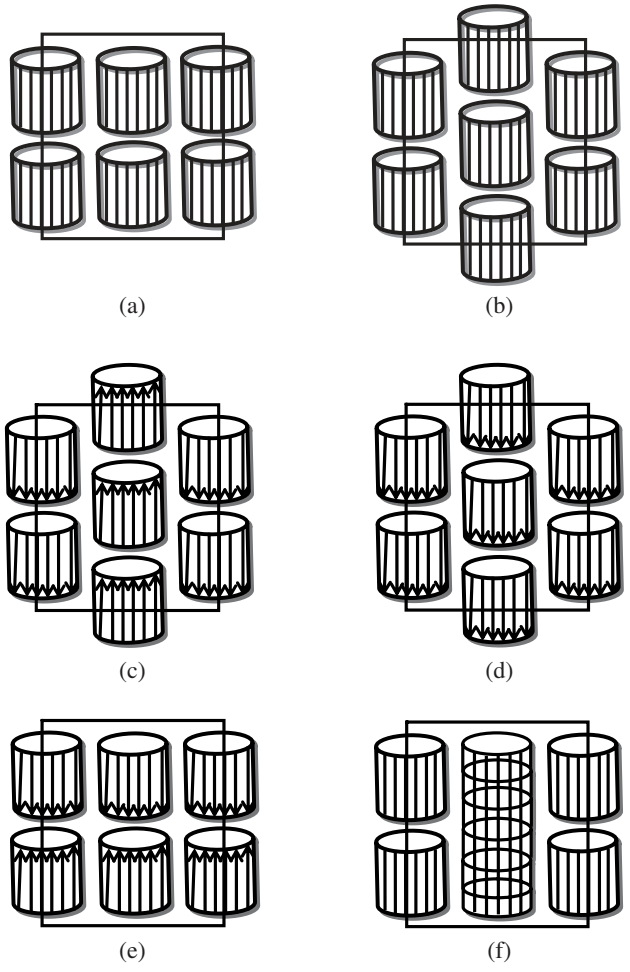

Figure 19: Packing of HA2 in the unit cell. (a) View perpendicular to long *c* axis. (b) View down the *c* axis.

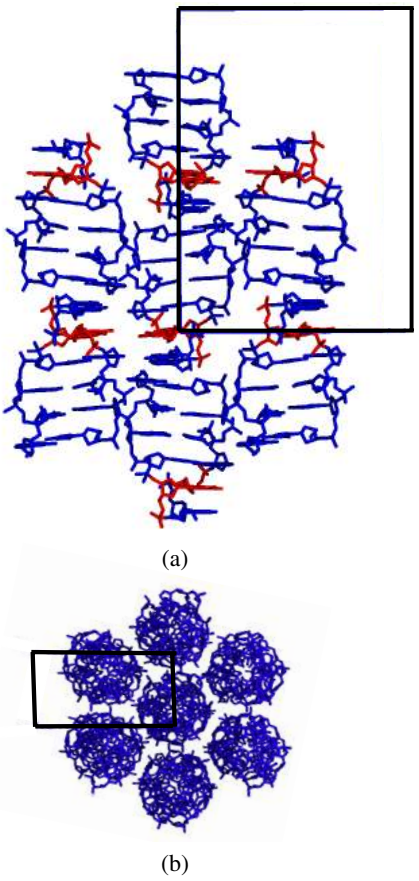

hexagonal $P6_5$. The packing of the helices in the orthorhombic crystal is very similar to that in HA2 as well as $d(CGCGCG)_2$ (Figure 21). Cobalt hexammine ions, which were clearly visible in the electron density map, are probably responsible in this case for maintaining the integrity of the specific packing mode. A lowering of the concentration of the ion leads to insufficient ions to maintain the packing, and therefore the hexagonal packing mode. In the hexagonal crystals, the cell dimensions expand to accommodate two helical columns in the projection of the asymmetric unit on to the *ab* plane (Figure 22). One of these columns is placed on the 6_5 screw along the *c* axis. It follows from this, from the *c* axis of about 45 Å, and from the inherent 6_5 screw symmetry in Z-DNA, that the single complete helix occupying the *c* axis is in fact generated by the six-fold screw applied to a dinucleotide. Owing to lack of perfect symmetry in the sequence (i.e. the presence of the A.T base pair) as well due to probable micro-structural heterogeneities, the helix generated by the six-fold is disordered. The asymmetric unit thus consists of one hexamer duplex and a dinucleotide duplex, the latter being positioned on the 6_5 screw axis. The crystallographic symmetry operators then generate the infinite columns of helices that make up the crystal. To summarize, a lowering of the concentration of the ion that binds the helices together leads to disorder in alternate columns of

Figure 20: Packing of HA4 in the space group $P2_1$. (a) View perpendicular to long c axis. (b) View down the c axis.

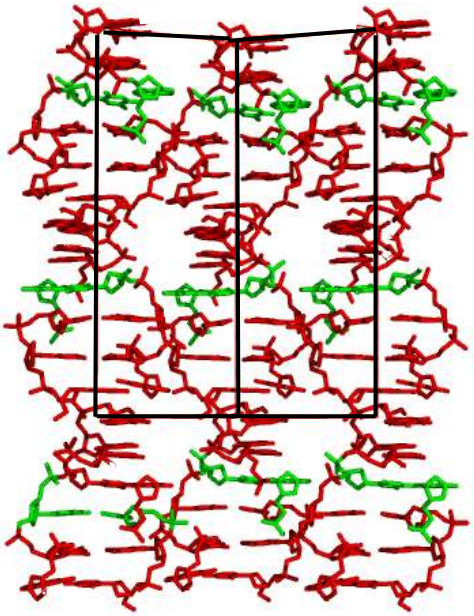

(a)

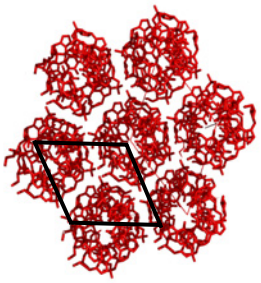

(b)

Figure 21: Packing of HA6 in the orthorhombic space group $P2_12_12_1$. (a) View perpendicular to long c axis. (b) View down the c axis.

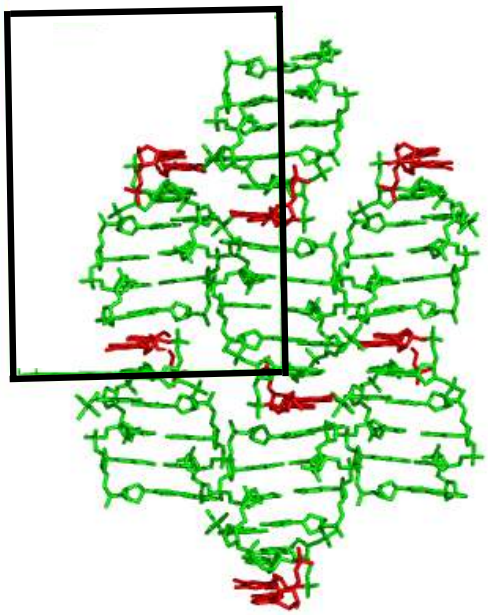

(a)

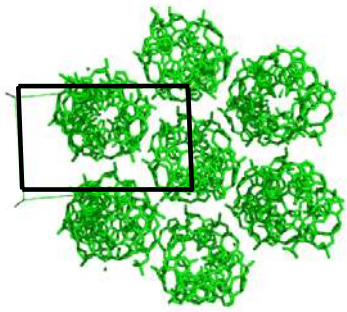

(b)

helices, which in turn leads to the hexagonal packing mode. An interesting byproduct is the formation, occasionally, of ring-shaped crystals (Figure 23) at lower ion concentrations (Satheesh and Gautham, 1999). However, except for the lowering of the packing integrity of the helices in the crystals, there is no clear explanation that could link the nanoscopic changes in the crystal packing to the formation of these micron-sized rings.

The non-alternating sequence $d(CCCGGG)_2$ crystallizes in the space group $P2_12_12_1$, in what may be called the standard Z-DNA unit cell. In attempts to improve data quality, which was poor beyond 3 Å, fresh crystals of this sequence were grown. While these crystals too did not diffract well beyond 3 Å, the data indicated either a hexagonal or monoclinic cell. However the reciprocal lattice showed no hexagonal symmetry. To decide between the two cells, the data were processed in a triclinic cell and the R_{merge} for equivalent reflections was calculated in the two possible systems. The values were 0.12 and 0.35 for 4414 and 1869 reflections in the monoclinic and hexagonal systems respectively. Analysis of the residuals in different resolution shells also showed that the values were better in the monoclinic systems. The lack of systematic absences helped fix the space group as P2 with c as the unique axis, $Z = 8$. Both this monoclinic system, as well the orthorhombic system seen in the first set of crystals can occur on the basis of approximately the same packing mode. The only difference is that in the monoclinic system the terminal base pairs of

Figure 22: Packing of HA6 in the hexagonal space group $P6_5$. (a) View perpendicular to long *c* axis. (b) View down the *c* axis.

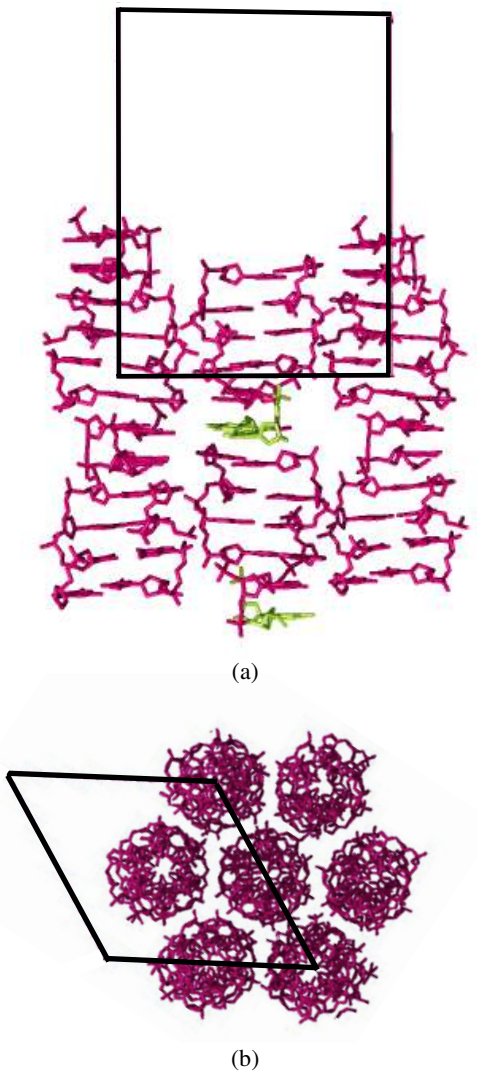

Figure 23: Ring crystal. The bar indicates 70 microns.

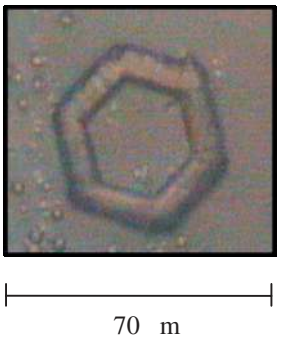

the hexamers in adjacent helical columns lie on the same plane.

The decamer sequences $d(CGCGTACGCG)_2$ and $d(CGGGCGCCCG)_2$, and the tetradecamer sequence $d(CGCGCGTACGCGCG)_2$ (P.K. Mandal, S. Vengadesh and N. Gautham, 2008, unpublished results) demonstrate interesting variants of the 'bundles of columns of helices' mode of packing. The decamer has one dinucleotide step less than the six dinucleotides (twelve base pairs) required to complete one full turn of the Z helix, while the tetradecamer has one extra dinucleotide step. Both sequences assumed the canonical Z type helical structure as well as crystal packing. Thus the decamer helices are stacked one over the other to form infinite helical columns that are then bundled together to form the crystal. However, the crystal unit cell along the *c* axis of about 45 Å accommodates twelve base pairs, i.e. one complete turn of the Z helix. In the case of the hexamers this requirement was satisfied by arranging two hexamers along the axis. For the decamer the requirement is satisfied by 'borrowing' a dinucleotide step from the next helix to make up the dozen base pairs. Repetition of this pattern leads to the next unit cell having to 'borrow' two dinucleotides from the one succeeding it, and so on until six decamers constitute five unit cell displacements along the long *c* axis (Figure 24). The space group is $P6_5$ and the decamer sits on the 6_5

Figure 24: Six decamers span five unit cells. Each unit cell accommodates twelve base pairs. The helical axis is parallel to the *c* axis.

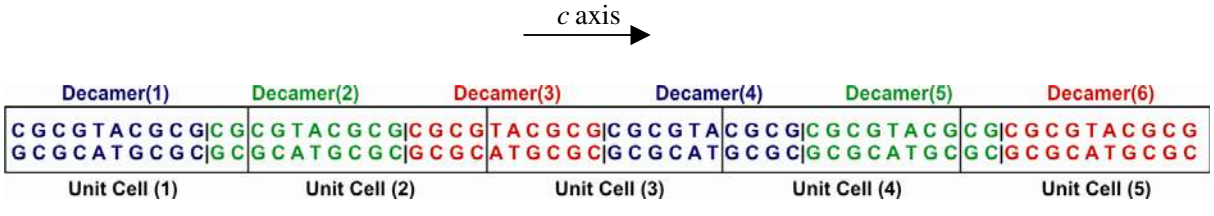

Figure 25: Six tetradecamers span seven unit cells. Each unit cell accommodates twelve base pairs. The helical axis is parallel to the *c* axis.

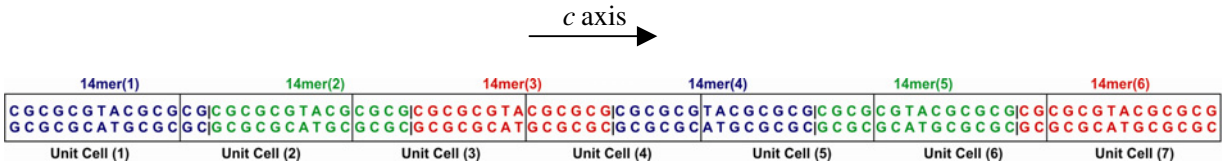

screw axis. This leads nominally to a dinucleotide as the asymmetric unit. Owing to the decameric sequence, this dinucleotide has the sequence $d(CG)_2$ in 80% of the cases, and the sequence $d(TA)_2$ in the other 20% of the cases. The decameric sequence $d(CGGGCGCCCG)_2$ packs in a similar fashion, with six duplexes occupying five unit cells. Again the decamer sits on the crystallographic screw axis. The space group however is now $P3_2$ and the asymmetric unit is nominally a tetramer, with the dodecamer required to complete one turn of the Z-helix being generated by the operation of the three-fold screw. There are two tetramer sequences, $d(CGCG)_2$ with 80% occupancy and $d(GCGC)_2$ with 20% occupancy. A tetramer is also the asymmetric unit in crystals of the tetradecamer $d(CGCGCGTACGCGCG)_2$, which takes up the space group $P3_2$. In these crystals six 14-mers span 7 unit cells (Figure 25), and the tetramer in the asymmetric unit has the sequences $d(CGCG)_2$, d(CGTA).(TACG) and d(TACG).(CGTA) with 72, 14 and 14% occupancies respectively. The exact nature of the interhelical interactions and perhaps the metal ion interactions that drive these variations in packing is not clear from the structures. In some cases, however, it is obvious from the structure that the metal ions play an important role in bringing about particular modes of packing.

Ion interactions:

Metal ion coordination to nucleic acids is not only required for charge neutralization, but is also essential for the biological function of nucleic acids. Nucleic acids contain four different potential sites of binding metal ions; the negatively charged phosphate oxygen atoms, the ribose hydroxyls, the base ring nitrogen and the exocyclic base keto groups (Ahrland *et al.*, 1958; Pearson, 1966). Metal ions, however can also have a destabilizing effect on DNA double helical structure if they interact with bases rather than with phosphate groups (Eichhorn *et al.*, 1968). The interaction of hexamine ions with DNA is of particular interest because these ions strongly induce a transition from right handed B-type to left handed Z-type (Thomas and Messner, 1988; Gueron *et al.*, 2000).

The HA2 sequence, d(CACGCG).d(CGCGTG), was crystallized using Mg^{2+} as the counter ion.

Figure 26: Cobalt hexammine ion interactions with neighbouring helices in the orthorhombic crystals of HA6. The electron density net is drawn at 1.2σ level. The dotted lines represent hydrogen bonds.

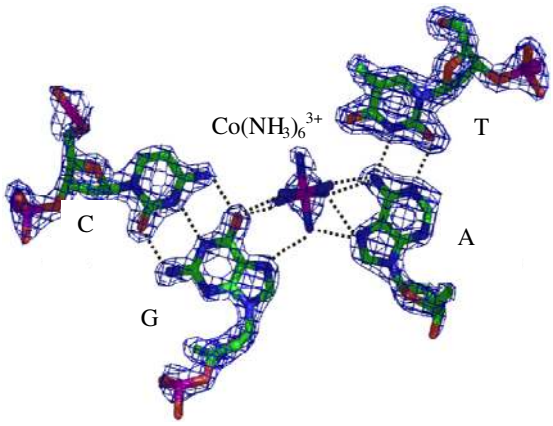

Figure 27: Ruthenium hexammine ion interactions with neighbouring helices in the orthorhombic crystals of HA6. The electron density net is drawn at 1.0σ level. The dotted lines represent hydrogen bonds.

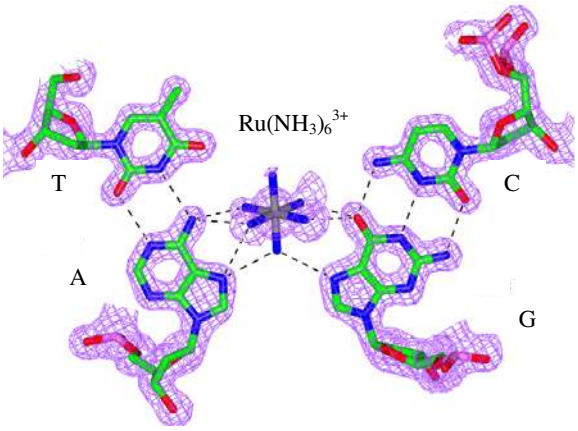

As described above, this sequence adopts the standard Z-DNA structure. The Mg ions could not be identified in the electron density maps. This led to the conclusion that the role of the ion in these crystals is a non-specific one. The same sequence was also crystallized in the presence of $[Ru(NH3)_6]^{3+}$ions, and without any Mg. Once again the structure was close to the standard Z DNA model. The only noticeable differences were in the values of the twist, which showed that the pyrimidine-purine steps in ruthenium structure are slightly overwound as compared to the magnesium structure. Also the values of x-displacement are somewhat higher in the ruthenium structure, indicating a shift of the base pairs away from the helix axis into the major groove. Like the magnesium ions, the ruthenium hexammine ion could not be identified in the electron density map. Thus either the ion does not enter the crystal lattice, or does so only in the bulk solvent, and makes no specific interactions with the DNA. These two ions, therefore, play a non-specific role in stabilizing the structure and the crystal packing, with their charge-neutralization activity probably mediated by labile water molecules.

The HA6 sequence, d(CGCGCA).d(TGCGCG), was crystallized complexed with both cobalt hexammine chloride and ruthenium hexammine chloride. In both cases crystals grew in two different habits that could be indexed in two different space groups, orthorhombic and hexagonal. As described above, a slight change in the ion concentrations leads to changes in the inter-helical interactions that probably result in different space groups. In both the cobalt and ruthenium structures, and both in the orthorhombic structure as well as the hexagonal one, the hexammine ion makes specific contacts with the single adenine base as well with the guanine bases in the neighbouring helix (Figures 26 and 27). In the orthorhombic structure, in the presence of either metal ion, this interaction induces a tautomeric shift from amino adenine to imino group adenine (Thiyagarajan *et al.*, 2004, Bharanidharan *et al.*, 2007), and consequently results in a 'wobble' A:T base pair. In the hexagonal space group, there is no such wobble base pair discernible. As described previously, the backbone is a mixture of Z_I and Z_{II} conformations in the orthorhombic crystals in both the cobalt and ruthenium structures. However these conformational variations are not correlated with the ion interactions.

Acknowledgements

We thank the following agencies of the Government of India for funding the projects under which the work reported here was carried out: DST, DBT and UGC. We thank the University of Madras for infrastructural and administrative support. We thank all our colleagues and collaborators, in particular Prof. S.S. Rajan, for discussion, encouragement and assistance. PKM thanks CSIR for the JRF.

Received 27 May 2008; revised 27 August 2008.

References

1. Ahrland, S., Chatt, J., and Davies, N.K. (1958). The relative affinities of ligand atoms for acceptor molecules and ions. *Quart. Rev. Chem. Soc.* **12**, 265–276.
2. Bharanidharan, D. (2007). X-Ray crystal structure and theoretical studies on nucleic acid sequences, Ph.D thesis, 26–34, University of Madras.
3. Bharanidharan, D., Thiyagarajan, S., and Gautham, N. (2007). Hexammine ruthenium (III) ion interactions with Z-DNA. *Acta Cryst.*, **F63**, 1008–1013.

4. Chevrier, B., Dock, A.C., Harmann, B., Leng, M., Moras, D., Thuong, M.T., and Westhof, E. (1986). Solvation of the left-handed hexamer d(5BrC-G-5BrC-G-5BrC-G) in crystals grown at two temperatures. *J. Mol. Biol.* **188**, 707–719.
5. Crawford, J. L., Kolpak, F. J., Wang, A. H.-J., Quigley, G. J., van Boom, J.H., van der Marel, G., and Rich, A. (1980). The tetramer d(CpGpCpG) crystallizes as a left-handed double helix. *Proc. Nat. Acad. Sci., U.S.A.* **77**, 4016–4020.
6. Dickerson, R.E. (1992). DNA structures from A to Z. *Methods Enzymol.* **211**, 67–111.
7. Drew, H.R., and Dickerson, R.E. (1981). Structure of B-DNA dodecamer. III. Geometry of hydration. *J. Mol. Biol.* **151**, 535–556.
8. Drew, H.R., Dickerson, R.E., and Itakura, K. (1978). A salt-induced conformational change in crystals of the synthetic DNA tetramer d(CpGpCpG). *J. Mol. Biol.* **125**, 535–543.
9. Drew, H.R., Takano, T., Tanaka, S., Itakura, K., and Dickerson, R. E. (1980). High-salt d(CpGpCpG), a left-handed Z′ DNA double helix. *Nature* **286**, 567–573.
10. Drew, H.R., Wing, R.M., Takano, T., Broka, C., Tanaka, S., Itakura, K., and Dickerson, R.E. (1981). Structure of a *B*-DNA dodecamer: Conformation and dynamics. *Proc. Natl. Acad. Sci. U.S.A.* **78**, 2179–2183.
11. Eichhorn, G.L., and Shin, Y.A. (1968). Interaction of metal ions with polynucleotides and related compounds. XII. The relative effect of various metal ions on DNA helicity. *J. Amer. Chem. Soc.* **90**, 7323–7328.
12. Franklin, R.E., and Gosling, R.G. (1953). Evidence for 2-chain helix in crystalline structure of sodium deoxyribonucleate. *Nature* **172**, 156–157.
13. Fujii, S., Wang, A. H.-J., van der Marel, G., van Boom, J. H., and Rich, A. (1982). The octamers d(CGCGCGCG) and d(CGCATGCG) both crystallize as *Z*-DNA in the same hexagonal lattice. *Nucl. Acids Res.* **10**, 7879–7892.
14. Gautham, N., Karthe, P., and Krishnaswamy, S. (1999). The effect of non-alternating sequences on the structure of left-handed Z-DNA. In *Perspectives in Structural Biology*. M. Vijayan, N. Yathindra, A. Kolaskar (Eds), pp 593–601. Indian Academy of Sciences, Universities Press, Hyderabad.
15. Gueron, M., Demaret, J.P., and Filoche, M. (2000). A unified theory of the B-Z transition of DNA in high and low concentrations of multivalent ions. *Biophys J.* **78**, 1070–1083.
16. Harper, N.A., Brannigan, J.A., Buck, M., Lewis, R.J., Moore, M.H., and Schneider, B. (1998). The structure of d(TGCGCA)2 and a comparison to other DNA hexamers. *Acta Cryst.*, **D54**, 1273–1284.
17. Herbert, A., and Rich, A. (1996). The Biology of Left-handed Z-DNA. *J. Biol. Chem.* **271**, 1155–1159.
18. Ho, P.S., and Mooers, B.H.M. (1997). Z-DNA crystallography. *Biopolymers* **44**, 65–90.
19. Jaworski, A., Hsieh, W.T., Blaho, J.A., Larson, J.E., and Wells, R.D. (1987). Left-handed DNA *in vivo. Science* **238**, 773–777.
20. Jayaraman, S., and Yathindra, N. (1981). Analysis of possible helical structures for poly (dinucleotides): evidence for left-handed *Z*-DNA and Z-type helices. *Curr. Sci.* **50**, 54–61.
21. Karthe, P. (1997). X-Ray crystallographic studies of nucleic acid components, Ph.D thesis, 19-51, University of Madras.
22. Klysik, J., Zacharias, W., Galazka, G., Kwinkowski, M., Uznanski,B., and Okruszek, A. (1988). Structural interconversion of alternating purine-pyrimidine inverted repeats cloned in supercoiled plasmids. *Nucl. Acids Res.* **16**, 6915–6933.
23. Langridge, R., Seeds, W.E., Wilson, H.R., Hooper, C.W., Wilkins, H.F., and Hamilton, L.D. (1957). Molecular Structure of Deoxyribonucleic Acid (DNA) *J. Biophys. Biochem. Cytol.* **3**, 767–778.
24. Malinina, L., Tereshko, V., Ivanova, E., Subirana, J.A., Zangrova, V., and Nekrasov, Y. (1998). Structural variability and new intermolecular interactions of Z-DNA in crystals of d(pCpGpCpGpCpG). *Biophys. J.* **74**, 2482–2490.
25. McLean, M.J., Blaho, J.A., Kilpatrick, M.W., and Wells, R.D. (1986). Consecutive A F255> T pairs can adopt a left-handed DNA structure. *Proc. Natl. Acad. Sci.* U.S.A. **83**, 5884–5888.
26. Möller, A., Nordheim, A., Kozlowski, S.A., Patel, D.J., and Rich A. (1984). Bromination stabilizes poly(dG–dC) in the Z-DNA form under low salt conditions. *Biochemistry* **23**, 54–62.
27. Parkinson, G.N., Arvanitis, G.M., Lessinger, L., Ginell, S.L., Jones, R., Gaffney, B., and Bernnan, H.M. (1995). Crystal and molecular structure of a new Z-DNA crystal form: d[CGT(2-NH2-A)CG] and its platinated derivative. *Biochemistry* **34**, 15487–15495.
28. Pearson, R.G. (1966). Acids and bases. *Science,* **151**, 172–177.
29. Peck, L.J., Nordheim, A., Rich, A., and Wang, J.C. (1982). Flipping of cloned d(pCpG)n d(pCpG)n DNA sequences from right- to left- handed helical structure by salt, Co(III), or negative supercoiling. *Proc. Natl. Acad. Sci. U. S. A.* **79**, 4560–4564.
30. Pohl, F.M., and Jovin, T.M. (1972). Salt induced co-operative conformational change of a synthetic DNA: Equilibrium and kinetic studies with poly(dG-dC). *J. Mol. Biol.* **67**, 375–396.
31. Rich, A., Nordheim, A., and Wang, A.H.-J. (1984). The chemistry and biology of left-handed Z-DNA. *Annu Rev Biochem.* **53**, 791–846.
32. Sadasivan, C., and Gautham, N. (1995). Sequence-dependent microheterogeneity of Z-DNA: The crystal and molecular structures of d(CACGCG)·d(CGCGTG) and d(CGCACG)·d(CGTGCG). *J. Mol. Biol.* **248**, 918–930.
33. Sadasivan.C., Karthe.P., and Gautham.N. (1994). Space group degeneracy in the packing of a non-selfcomplementary Z-DNA hexamer. *Acta Cryst.*, **D50**, 192–196.
34. Satheesh Kumar, P., and Gautham, N. (1999). Unusual ring-shaped oligonucleotide crystals. *Curr. Sci.* **77**, 1076–1078.
35. Schroth, G.P., Chou, P.J., and Ho, P.S. (1992). Mapping Z-DNA in the human genome. Computer-aided mapping reveals a nonrandom Z-DNA-forming sequences in human genes. *J. Biol. Chem.* **267,** 11846–11855.
36. Sinden R.R., 1994. Left-handed Z-DNA. In *DNA Structure and Function*. New York, Academic Press.
37. Singleton, C. K., Klysik, J., Stirdivant, S.M., and Wells, R.D. (1982). Left-handed Z-DNA is induced by supercoiling in physiological ionic conditions. *Nature* **299**, 312–316.
38. Subirana, J.A., and Solar-Lopez, M. (2003). Cations as hydrogen bond donors: a view of electrostatic interactions in DNA. *Annu. Rev. Biophys. Biomol. Struct.* **32**, 27–45.
39. Sutherland, J.C., Griffin, K.P., Keck, P.C., and Takacs, P.Z. (1981). *Z*-DNA: Vacuum ultraviolet circular dichroism. *Proc. Nat. Acad. Sci., U.S.A.* **78**, 4801–4804.
40. Thiyagarajan, S., Rajan, S.S., and Gautham, N. (2005). Structure of d(TGCGCG). d(CGCGCA) in two crystal forms: effect of sequence and crystal packing in Z-DNA. *Acta Cryst.*, **D61**, 1125–1131.
41. Thiyagarajan, S., Rajan, S.S., and Gautham, N. (2004). Cobalt hexammine induced tautomeric shift in Z-DNA: the structure of d (CGCGCA).d(TGCGCG) in two crystal forms. *Nucl. Acid Res.* **32**, 5945–5953.
42. Thiyagarajan, S., Satheesh Kumar, P., Rajan, S.S., and Gautham, N. (2002). Structure of $d(TGCGCA)_2$ at 293K: comparison of the effects of sequence and temperature. *Acta Cryst.*, **D58**, 1381–1384.
43. Thomas, T.I., and Messner, R.P. (1988). Hexammine ruthenium (III) chloride: a highly efficient promoter of the B-DNA to Z-DNA transition of poly-(dG-m5dC).poly(dG-m5dC) and poly(dG-dC).poly(dG-dC). *Biochimie* **70**, 221–226.
44. Wang, A.H.-J., Quigley, G.J., Kolpak, F.J., Crawford, J.I., van Boom, J.H., van der Marel, G., and Rich, A. (1979). Molecular structure of a left-handed double helical DNA fragment at atomic resolution. *Nature* **282**, 680–686.
45. Wang, A.H.-J., Quigley, G.J., Kolpak, F.J., van der Marel, G.,

van Boom, J.H., and Rich, A. (1981). Left-handed double helical DNA: Variations in the backbone conformation. *Science* **211**, 171–176.
46. Watson, J.D., and Crick, F.H.C. (1953). Molecular structure of nucleic acids: A structure for deoxyribose nucleic acid. *Nature* **171**, 737–738.
47. Weaire, D. (1996). The Kelvin Problem, Foam Structures of Minimal Surface Area, Taylor and Francis, London.
48. Wing, R., Drew, H., Takano, T., Broka, C., Tanaka, S., Itakura, K., and Dickerson, R.E. (1980). Crystal structure analysis of a complete turn of B-DNA. *Nature* **287** (5784), 755–758.

N. Gautham After obtaining a Ph.D. from the Indian Institute of Science, N. Gautham joined the University of Madras, where he is now a Professor. His research interests are chiefly in Structural Biology and Bioinformatics. He has published 2 textbooks and more than 46 papers, in the area of DNA Crystallography and Bioinformatics and Computational Biology. He teaches several courses in the areas of X-ray Crystallography and Structural Biophysics and Bioinformatics. In 2007 he was elected Fellow, National Academy of Science, India. He has made significant contributions in the following areas of structural biology and bioinformatics - DNA structure, protein folding and structure prediction, and computational genomics. In DNA crystallography, he published the first oligonucleotide structure solved exclusively from within the country. This structure and subsequent ones extended the concept of sequence-specific DNA structure to the left-handed Z form. These studies also identified a novel 'wobble' A.T base pair. In protein structure, he has pioneered the use of the theory of experimental design in combination with mean field theory to explore the conformational space of molecules. This method has been used in de novo protein structure prediction.

Pradeep Kumar Mandal is a Junior Research Fellow (CSIR) in the Centre of Advanced Study in Crystallography and Biophysics, University of Madras, Chennai. He graduated with B.Sc Biotechnology Degree (2004) from the University of Kerala, Thiruvananthapuram and did his Masters in Life Sciences from Pondicherry University, Puducherry. His areas of interest include DNA crystallography, Crystal morphologies, Cell signaling and Proteomics.

S. Venkadesh is a Junior Research Fellow (DST) in the Centre of Advanced Study in Crystallography and Biophysics, University of Madras, Chennai. He did his Bachelors in Science (2002) from Madurai Kamaraj University, Madurai and Masters Degree in Physics from Alagappa University, Karaikudi. His research interest includes DNA nanostructures and Nano-electronics